RESEARCH ARTICLE

Short-term evolution pattern in salt marsh landscapes: the importance of physical constraints

Liming Xue · Tianyou Li · Xiuzhen Li · **Yuxin Bi · Lin Su · Yuanhao Song ·
Wenzhen Zhao · Jianzhong Ge · Qing He · Benwei Shi**

Abstract

Context Salt marsh landscapes at the land-sea interfaces exhibit contrasting spatiotemporal dynamics, resulting from varying physical constraints that limit new marsh establishment. The expansion of salt marsh landscapes towards the sea or their retreat towards the land is determined by patch-level changes, relying on the balance of power between the intrinsic biota traits and external physical disturbances.

Objectives Examine how marsh dynamics respond to physical constraints, and clarify the pathway from coupled physical processes involving hydrodynamic forces, sediment transport, and morphological changes to rapid patch evolution and landscape changes.

Methods We defined and distinguished four types of marsh changes based on patch proximities from five-month drone images in two typical marsh pioneer zones of the Yangtze Estuary, China: outlying expansion, edge expansion, infilling expansion, and retreat. Hydrodynamics and sediment transport were synchronously measured and compared near the two marsh edges, and morphological changes were generated by drone-derived digital elevation models (DEMs).

Results We identified distinct seasonal patterns of net marsh expansion at the accretion-prone site, that is: Net marsh expansion started from the outlying expansion in spring, followed by edge expansion in summer and infilling expansion in autumn. However, at the erosion-prone site that experienced high bed shear stress, low sediment availability and high seaward sediment transport, we only observed limited infilling and edge expansion in spring. This suggests that the potential for long-distance patch formation beyond the initial marsh edges is diminished in areas subjected to intensive physical disturbances.

Conclusions Patch evolution dynamics in response to site-specific physical constraints drive state differentiation of salt marsh landscape changes. Consequently, the heterogeneous evolution in salt marsh landscapes should be taken into account in restoration practice.

L. Xue · T. Li · X. Li (✉) · Y. Bi · L. Su · Y. Song · W. Zhao · J. Ge · Q. He · B. Shi
State Key Laboratory of Estuarine and Coastal Research, Institute of Eco-Chongming, East China Normal University, 500 Dongchuan Road, Shanghai 200241, People's Republic of China
e-mail: xzli@sklec.ecnu.edu.cn

X. Li
Yangtze Delta Estuarine Wetland Ecosystem Observation and Research Station, Ministry of Education & Shanghai Science and Technology Committee, Shanghai, People's Republic of China

Introduction

Salt marshes are one of the most valuable ecosystems on the earth (de Groot et al. 2012). Ecosystem services sustained by salt marshes play key roles in human welfare, biogeochemical cycles and biodiversity conservation (Costanza et al. 1997; Kirwan and Mudd 2012; Bauer et al. 2013; Temmerman et al. 2013). Nevertheless, with the combined effect of sea level rise (Church and White 2011), decreased sediment supply (Syvitski et al. 2005; Kondolf et al. 2014;), extreme events (Woodruff et al. 2013; Vasseur et al. 2014; Hanley et al. 2020) and estuarine projects (Luan et al. 2018), salt marshes worldwide are facing threats, and their deterioration is accelerating (Kirwan and Megonigal 2013; Li et al. 2018; Schuerch et al. 2018). Thus, an in-depth understanding of salt marsh evolution is needed to incorporate interdisciplinary solutions linking land cover and environmental processes.

Time scale matters in marsh evolution. Shifts of marsh cover in pioneer zones often happen within a few months due to the short life history of marsh macrophytes (Jiang et al. 2022), and becomes an essential portion of cyclic marsh-mudflat dynamics (Bouma et al. 2016). Previous studies have made efforts to fill the gap between the annual or decadal marsh changes, and physical constraints (e.g., van Wesenbeeck et al. 2008; Wang and Temmerman 2013; van Belzen et al. 2017). However, spatially explicit short-term marsh evolution (usually within a few months) is poorly understood and limited by the resolution of data acquisitions.

Spatially scaling up amplifies the complexities of marsh development (van de Koppel et al. 2012; Folkard 2019). The equilibrium between marsh vegetation and sediment dynamics at population-community level is the prerequisite for marsh survival (Ge et al. 2019). At the landscape level, unique land covers are created as a result of spatial heterogeneities in environmental factors (Perry 2002; Moffett et al. 2012; Stein et al. 2014). Site-specific variables such as sediment supply and geomorphology may result in distinct trajectories of marsh development (Mariotti and Carr 2014; Schuerch et al. 2014; Li et al. 2021). Additionally, infrequent but abrupt disturbances (e.g., storms and peak riverine runoffs) bring uncertainties to marsh evolution (Wang et al. 2016; Leonardi et al. 2018). Therefore, it is necessary to explore how salt marshes spatially respond to the diverse and intertwined physical constraints, as this will help in understanding the variety of salt marsh landscapes.

Dynamic salt marsh landscapes are formed through the life-history processes of pioneer species that depend on biophysical interactions, including propagule retention (Zhu et al. 2020), seedling establishment (Zhao et al. 2021c), and clonal growth (Huang et al. 2022). Yuan et al. (2020) suggested that successful colonization of pioneer species require a suitable elevation and a moderate sedimentary regime. Other studies have also emphasized the importance of bed level changes in marsh establishment (e.g., Bouma et al. 2016; Cao et al. 2018; Wiegman et al. 2018). To a large extent, hydrodynamic force and sediment supply control the local accretion-erosion shifts. Less intensive hydrodynamics and high sediment availability promote marsh expansion (Ladd et al. 2019), while erosion induced by strong hydrodynamics and low sediment supply can lead to marsh loss (Poirier et al. 2017; Willemsen et al. 2022). Given the significance of physical settings, the spatially varying external forces such as sediment dynamics and morphodynamics may make uneven effects on marsh development, and contribute to the differentiation of short-term marsh evolution patterns at the landscape scale.

Here, we aim to unravel the underlying links between short-term marsh evolution patterns and physical constraints, taking typical marsh pioneer zones in the Yangtze Estuary as the model system (Fig. 1a, b). We conducted field investigations in two marsh pioneer zones subjected to similar wind and tide conditions (the straight-line distance between the two sites is about 7 km, Fig. 1c), with drone flights and hydro-sediment measurements in the five-month survey. We compared sediment dynamics, geomorphology, and marsh changes between the two sites, and further clarified the relationships between sediment dynamics, morphodynamics, and marsh dynamics. The outcomes of the present study will shed light on spatial consequences of biophysical interactions and give implications for restoration strategies of coastal wetlands in other similar mega-delta systems.

Site description

The Yangtze River flows in the length of 6379 km with a basin area of 1,800,000 km^2 (Dai 2021) before
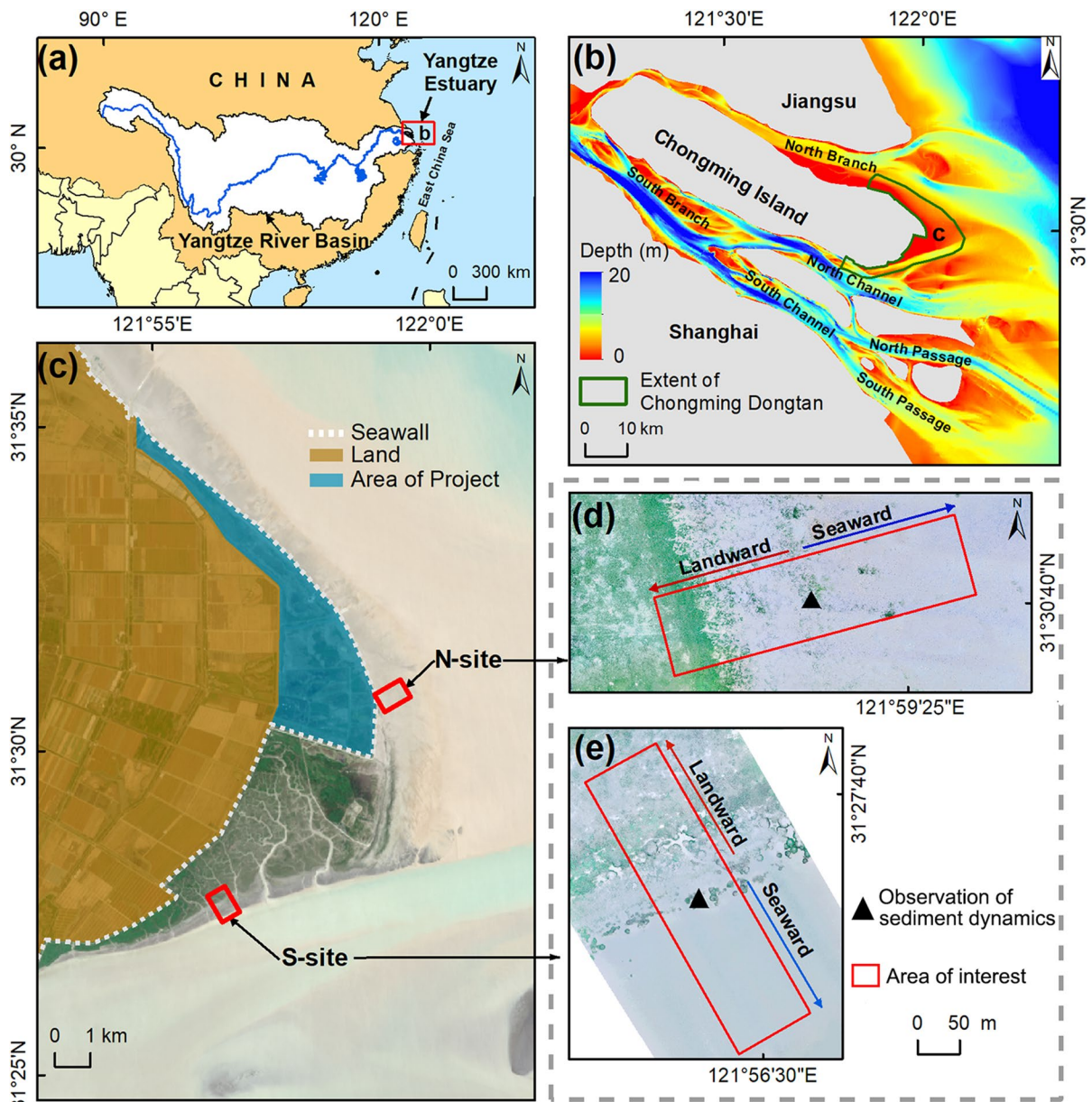
Fig. 1 Study area: **(a)** Extent of Yangtze River Basin and location of the Yangtze Estuary; **(b)** Overview of the Yangtze Estuary; **(c)** Satellite images of CDNR (data source: Landsat-8); **(d)** Drone images at N-site and **(e)** at S-site

entering the East China Sea (Fig. 1a). The Yangtze Estuary (Fig. 1b) is famous for bifurcated patterns and high turbidity as one of the mega estuarine systems worldwide. Due to hydraulic projects and the soil conservation policy in the Yangtze River Basin, sediment discharge into the Yangtze Estuary has started to decline since the 1970s (from > 400 Mt yr^{-1} in 1970 to 105 Mt yr^{-1} in 2019, Guo et al. 2019). The

continuously decreased fluvial sediment input has provoked concerns about the vulnerability of coastal wetlands in the Yangtze Estuary (Yang et al. 2006; Wang et al. 2014; Leonardi et al. 2021).

Chongming Dongtan National Nature Reserve (CDNR) is located at the east head of Chongming Island in the Yangtze Estuary (Fig. 1c). Astronomic tides in the region are semidiurnal with diurnal

inequality. The average tidal range is 2.5 m but can reach 3.5–4.0 m during spring tides according to the Sheshan gauging station (20 km east of CDNR, Yuan et al. 2022). Winds controlled by the subtropical monsoon prevail in the southeast in summer and the northwest in winter. Highly variable wind speed can reach 36 m s^{-1} (GSII 1996).

Two represented marsh pioneer zones were selected in CDNR, namely N-site and S-site, respectively (Fig. 1d, e). Properties of vegetation, surface sediment and water at both sites were shown in Table 1. The two sites were mainly covered by pioneer *Scirpus* communities (*Scirpus mariqueter* at N-site, and *Scirpus triqueter* at S-site). Surface sediment is muddy at N-site and sandy at S-site. Controlled by runoffs of the North Channel in the Yangtze Estuary (Fig. 1b), water salinity at S-site is lower than that at N-site. Vertical accretion at N-site has continued after the new seawall closure in 2014 (Fig. 1c, Wei et al. 2018), while erosion was found at S-site (Zhao et al. 2008; Yang et al. 2020).

Methodology

Data acquisition

Drone monitoring

The RTK-enabled drone (DJI Phantom 4-RTK, DJI, China) was equipped to take photos at N-site and S-site. The advantage of the RTK-enabled drone is its high accuracy without the need for ground control points. Four flights were executed on the following dates in 2021: 23rd April, 30th June, 31st July, and 24th September (see Table S1 for flight time). All flights used the same parameter settings, as detailed in Table S2.

Ground validation points were measured instantly after each flight using the real-time kinetics GPS units (RTK-GPS, Hi-Target, China). Validation points for April at the N-site were unavailable due to severe weather conditions. All surveys were horizontally georeferenced in China Geodetic Coordinate System 2000 (CGCS2000) and vertically georeferenced in the local Wusong datum.

Measurements of hydrodynamics and sediment

Waves (RBRduo^3 T.D| wave, RBR, Canada), currents (EMCM, JFE, Japan) and sediment (OBS-3A, Campbell Scientific, USA) were observed synchronously at the two marsh edges (Fig. 1b, e) in four spring tides from 8th to 10th June in 2021, with an average wind speed of 3.6 m s^{-1} (Fig. S1). All deployed sensors were placed at 15 cm above the seabed (Fig. S2). Turbidity signals recorded by OBS-3A were calibrated to suspended sediment concentration (SSC) using sediment samples near the instruments (Fig. S3).

Drone-related data processing

It took three steps in the procedure of drone-related data processing (Fig. S4): (1) Obtain orthoimages and rough point cloud; (2) Recognize marsh covers in orthoimages; (3) Modify point cloud and generate a digital elevation model (DEM). The procedure specified a spatial resolution of 10 cm. DEM products were validated against ground validating points and yielded low errors at both sites (4.34 cm at N-site and 4.60 cm at S-site, Fig. S5).

Data analysis

Spatial analysis on marsh evolution

We selected two proxies, the marsh area and the number of patches, respectively, to represent spatially explicit marsh vegetation dynamics. To elaborate,

Table 1 Properties of vegetation, sediment and water at N-site and S-site

Items	Properties	N-site	S-site
Vegetation	Species	*Scirpus mariqueter*	*Scirpus triqueter*
	Canopy height (m)	40.26±3.81	53.14±6.42
	Aboveground biomass (g m^{-2})	244.96±52.01	177.04±39.73
Sediment	Median grain size (ave.±std., µm)	17.48±7.75	43.20±4.50
Water	Salinity (median/max., PSU)	10.87/24.44	2.44/16.18

changes in the marsh area represent the extent of marsh vegetation gain or loss covering the landscape, while changes in the number of marsh patches explain how marsh vegetation patches are spatially rearranged (e.g., more clustered or more scattered).

By referencing theories and cases in urban growth (Forman 1995; Berling- Hoffhine Wilson et al. 2003; Berling-Wolff and Wu 2004; Xu et al. 2007; Liu et al. 2010), four types of marsh patch changes were defined and identified according to patch-to-patch proximities (Fig. 2): outlying expansion, edge expansion, infilling expansion and retreat.

Outlying expansion means isolated-grown patches apart from old patches. Edge expansion is defined as the growth adjacent to patch fringes. Infilling expansion refers to the new growth filling gaps inside or between old patches. Retreat is the reduction of patch area. The three marsh expansion topologies were distinguished from shared borders between newly-grown patches and existing patches, using the method proposed by Xu et al. (2007):
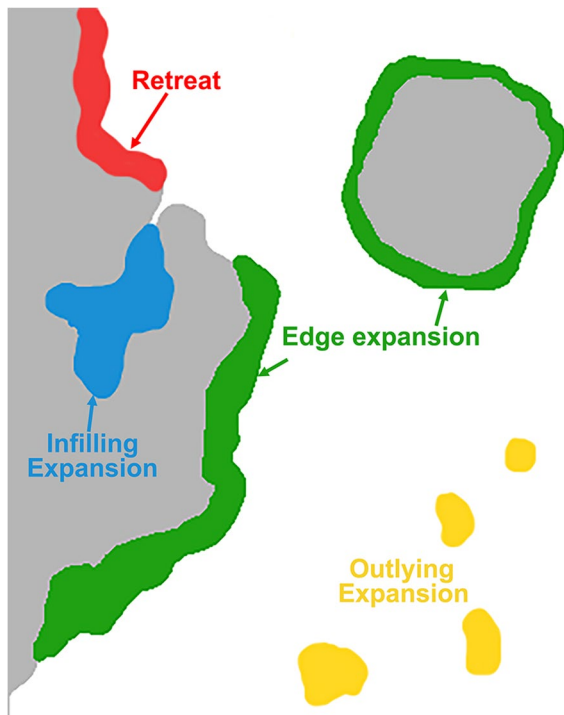
$$S = L_C/L \tag{1}$$

Fig. 2 Illustrations of marsh changes around the grown marshes (the gray part)

$$S = \begin{cases} = 0 & , outlying\,expansion \\ \in (0, 0.5) & , edge\,expansion \\ \in (0.5, 1] & , infilling\,expansion \end{cases} \tag{2}$$

where L_C is the length of the shared borders between new patches and old patches (m), L is the perimeter of new patches (m), and S is the ratio of " inherited borders" in newly grown patches.

Morphological changes

To assess the lateral propagation of tidal flats at the two sites, we used the dataset from the Sheshan gauging station to determine the mean high neap water level (MHNW) during the period from March to October 2021, with a value of 2.68 m above Wusong datum. The dynamic MHNW contour on the DEMs visually depicts the landward retreat or seaward expansion of tidal flats. Moreover, tidal flats below the MHNW were susceptible to inundation during most tides. In comparison, tidal flats above MHNW possibly would not be inundated by neap tides, thus gaining the opportunity for marsh seedlings to anchor and establish during the inundation-free period. Consequently, we computed the area of tidal flats (including both vegetated marshes and bare mudflats) above the MHNW as a proxy for potential habitats suitable for marsh establishment and growth.

We focused on vertical accretion or erosion on the tidal flats extending 200 m seaward from the initial marsh edges at both sites. To determine erosion/deposition rates, we subtracted DEMs from two neighboring months. To compare the accretion/erosion patterns between the two sites, we estimated the probability density function of monthly accretion rates over a five-month period. Additionally, we assessed elevation stability using the elevation standard deviation (STD) as a metric. This calculation followed the methodology by Xie et al. (2017), determining the STD for each spatial location over several months (specifically, in this study, four elevation values for calculating STD at each location).

Bed shear stress and sediment transport

In a calm, typhoon-free period, we collected in-situ data during four spring tides, including wave, current, and SSC measurements, which were utilized

to compute bed shear stress and sediment flux. Bed shear stress due to combined waves and currents (τ_{cw}, Pa) was estimated to quantify hydrodynamic forces (Equation S2-S12). Near-bed sediment flux per unit width within a specific duration was calculated and it was expressed as (Zhu 2017):

$$Q_s = \sum_{i=1}^{n} SSC_i V_i H \Delta t \tag{3}$$

where Q_s is sediment flux (kg m^{-1}), SSC is suspended sediment concentration (kg m^{-3}), V is current velocity values (m s^{-1}), Δt is the burst interval (600 s), n is the number of bursts, and H is the height of sensors above the seabed (0.15 m).

It assumed that sediment transport at the bottom 15 cm of the water column is landward in flooding stages and seaward in ebbing stages. Net sediment flux per tide was calculated as follows (Yang et al. 2020):

$$Q_{s-net} = Q_{s-flood} - Q_{s-ebb} \tag{4}$$

where Q_{net} is net sediment flux per tide (kg m^{-1} tide^{-1}) and positive in the landward direction, $Q_{s-flood}$ and Q_{s-ebb} refer to the sediment flux of flooding tides and ebbing tides, respectively.

Results

Spatiotemporal characteristics of salt marsh changes

Marshes at N-site expanded seaward, whereas those at S-site migrated landward during the surveyed five months (Fig. 3a). The marsh area at N-site grew from 4900 m^2 in April to 16,121 m^2 in September with a gradually compacted spatial structure over five months, while the marsh area at S-site decreased from 11,781 to 10,458 m^2 during the same period (Fig. 3b, c). At the stage of *Scirpus* establishment in spring (T1, from April to June), the number of patches at N-site increased explosively from 17 to 2874 but only 45 to 50 at S-site. Scattered patches at N-site quickly merged in summer (T2, from June to July) and contributed the greatest amount to marsh growth even though typhoon In-Fa attacked at the end of July (Fig. S6). Marshes at S-site began to shrink at the rate of 569 m^{-2} month^{-1} after typhoon In-Fa, resulting in an increased number of patches (from 50 to 148) due to fragmentation. Although the marsh area

at both sites decreased from summer to autumn (T3, July to September), marsh loss at S-site was 2.4 times quicker than that at N-site.

Distinctly different patch-level marsh changes were evident at the two sites (Fig. 3d). At N-site, marshes exhibited varying patterns of expansion throughout seasons, that was: from outlying expansion in spring (T1), to edge expansion in summer (T2), and to infilling expansion in autumn (T3). Conversely, the dominant pattern at the S-site shifted from infilling and edge expansion in spring (T1) to subsequent retreat following the impact of typhoons (T2 and T3).

Lateral propagation and vertical accretion-erosion of tidal flats

Tidal flats at S-site experienced obvious landward retreat, while N-site maintained more laterally stable tidal flats, as evidenced by the movement of MHNW at both sites (Fig. 4a). Similarly, the area of tidal flats above MHNW remained relatively stable at N-site but decreased at a rate of 1058 m^2 month^{-1} at S-site (Fig. 4b). These observations highlight that N-site provides a larger and more stable space along the sea-to-land gradient with a low inundation frequency, which is conducive to marsh survival, compared to S-site. Comparatively, S-site had narrow space for new marsh establishment beyond the initial marsh edge and this limited space was vulnerable to erosion.

S-site was generally more prone to erosion than N-site (Fig. 4c). Both sedimentary regimes were erosion-dominant because of typhoons but N-site was more prone to accretion. The erosion rate with the peak possibility was around 1.4 cm month^{-1} at N-site and approximately 7.5 cm month^{-1} at S-site. Besides, high elevation variabilities represented by elevation STD further explained that bed level at S-site was unstable (Fig. 4d). In summary, S-site experienced much more intensive erosion and variable bed level changes compared to N-site. These differences may be attributed to site-specific hydrodynamics and sediment availability.

Hydrodynamics and sediment transport near marsh edges

Marsh edges at S-site experienced stronger hydrodynamics and lower sediment availability than N-site (Fig. 5a-e). Among the observed four tides, maximum water depth (h), maximum significant wave
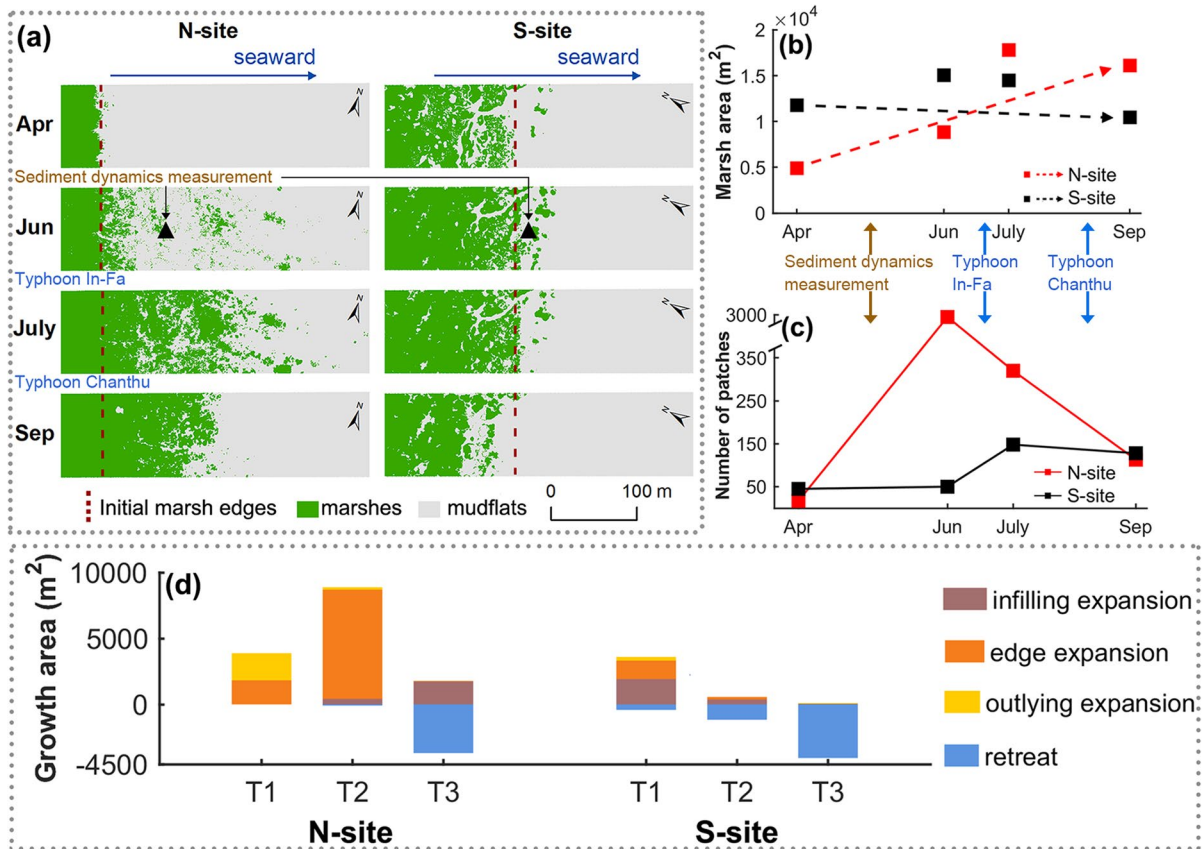
Fig. 3 Salt marsh changes at N-site and S-site: **(a)** Marsh cover; **(b)** Marsh area; **(c)** Number of patches; and **(d)** The growth area belonging to different change types in different periods. T1, T2 and T3 refer to the time interval from April to June, June to July and July to September, respectively

height (H_s) and mean flow velocity (V) at S-site were significantly 2.9, 3.6 and 1.8 times greater than those at N-site (Fig. 5a-c, $p < 0.01$, pairwise t-test), respectively. Intensive wave and current acted as significantly greater bed shear stress (τ_{cw}) at S-site (tide-averaged, 0.29±0.06 Pa), while 0.20±0.03 Pa at N-site (Fig. 5d, $p = 0.04$, two-sample t-test). Unlike differences in hydrodynamics between the two sites, SSC at S-site was significantly lower than that at N-site (tide-averaged, 3.22±0.19 kg m^{-3} at S-site and 4.07±0.28 kg m^{-3} at N-site, Fig. 5e, $p < 0.01$, pairwise t-test).

Sediment flux (Q_s) expressed that S-site had a higher magnitude of seaward-dominated sediment transport than N-site, within the range from -68.89 to 22.56 kg m^{-1} tide^{-1} at N-site and -187.20 to -67.19 kg m^{-1} tide^{-1} at S-site (Fig. 5f). The results proved that high τ_{cw} and low SSC significantly promoted seaward sediment

transport ($R^2 = 0.53$, $p = 0.04$ for the former, Fig. 5g; $R^2 = 0.75$, $p < 0.01$ for the latter, Fig. 5h). This implied that marsh edges with high bed shear stress plus low sediment availability (e.g., S-site in the study) would potentially be prone to being eroded due to weak sediment retention capacity.

Discussion

The present study aims to investigate how different physical constraints, including sediment dynamics and morphodynamics, influence seasonal marsh dynamics. This investigation was carried out by comparing two typical marsh pioneer zones in the Yangtze Estuary, China. Evidence from drone-based images reveals that all three types of the patch-level marsh expansion (outlying, edge, and infilling) were
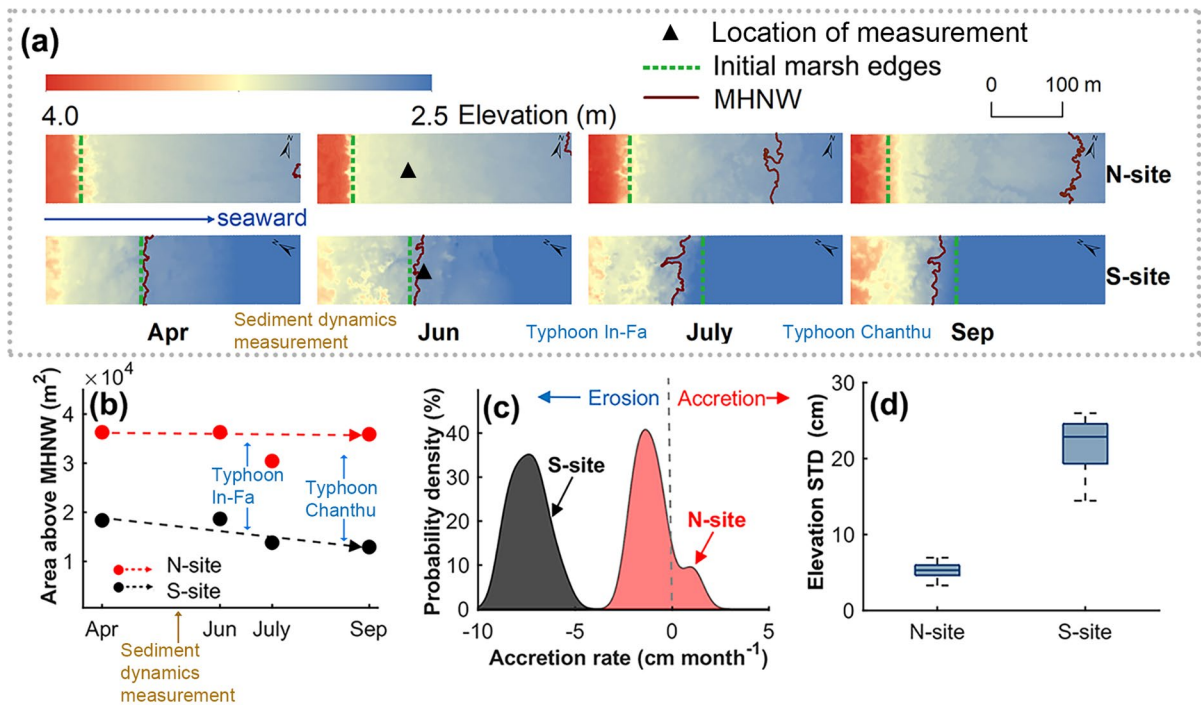
Fig. 4 Morphological changes at N-site and S-site: **(a)** Elevation distribution; **(b)** Change of area above MHNW; **(c)** Estimated probability density of accretion rate the 200-m seaward tidal flats beyond the initial marsh edge; and **(d)** Standard devi- ations among the four DEMs on the 200-m seaward tidal flats beyond the initial marsh edge. MHNW: mean high neap water level; STD: standard deviation

observed in the expanding marsh system (N-site). In contrast, in the retreating marsh system (S-site), only distance-limited infilling and edge expansion were evident. This finding underscore the significance of patch level marsh changes in sustaining and accelerating seasonal net marsh expansion, which is tightly associated with site-specific sediment dynamics and morphodynamics.

The shaping role of physical constraints in salt marsh establishment

Our results expressed that high bed shear stress plus low SSC decreased sediment retention capacity (Fig. 5g, h) and thus potentially accelerated vertical erosion near marsh edges. Theoretically, a high flow velocity can carry more sediment than a low one (Winterwerp, 2001). Low SSC can activate sediment resuspension by τ_{cw}-induced erosion to compensate the deficit in mass balance (Zhang et al. 2009; Debnath and Chaudhuri 2011). In addition, an increased sandy portion of surface sediment could weaken

sediment resistance to erosion by decreasing critical shear stress for erosion (τ_{ce}) (Panagiotopoulos et al. 1997). High τ_{cw} (Fig. 5d), low SSC (Fig. 5e), and sandy surface sediment (Table 1) at S-site increased erosion risks by increasing hydrodynamic forces and decreasing sediment erodibility. It was reasonable to infer that the bed level at S-site was more prone to being eroded and less stable than N-site from the four-tide observations, and the five-month morphological changes solidly evidenced this hypothesis (Fig. 4).

Strong hydrodynamics and unstable bed levels are effective signatures of physical disturbances to marsh establishment. Recent studies have revealed that the floatation of post-germinated seedlings promoted the onset of *Scirpus* quick dispersal (Zhao et al. 2021b; Jiang et al. 2022). The mechanism explained large-scale outlying expansion beyond existing marshes from April to June at N-site (Fig. 3d). Contrastingly, the limited outlying expansion at S-site (Fig. 3d) showed that a clear way from seedling floatation to the successful establishment depends on site-specific conditions. Physical disturbances induced by bed
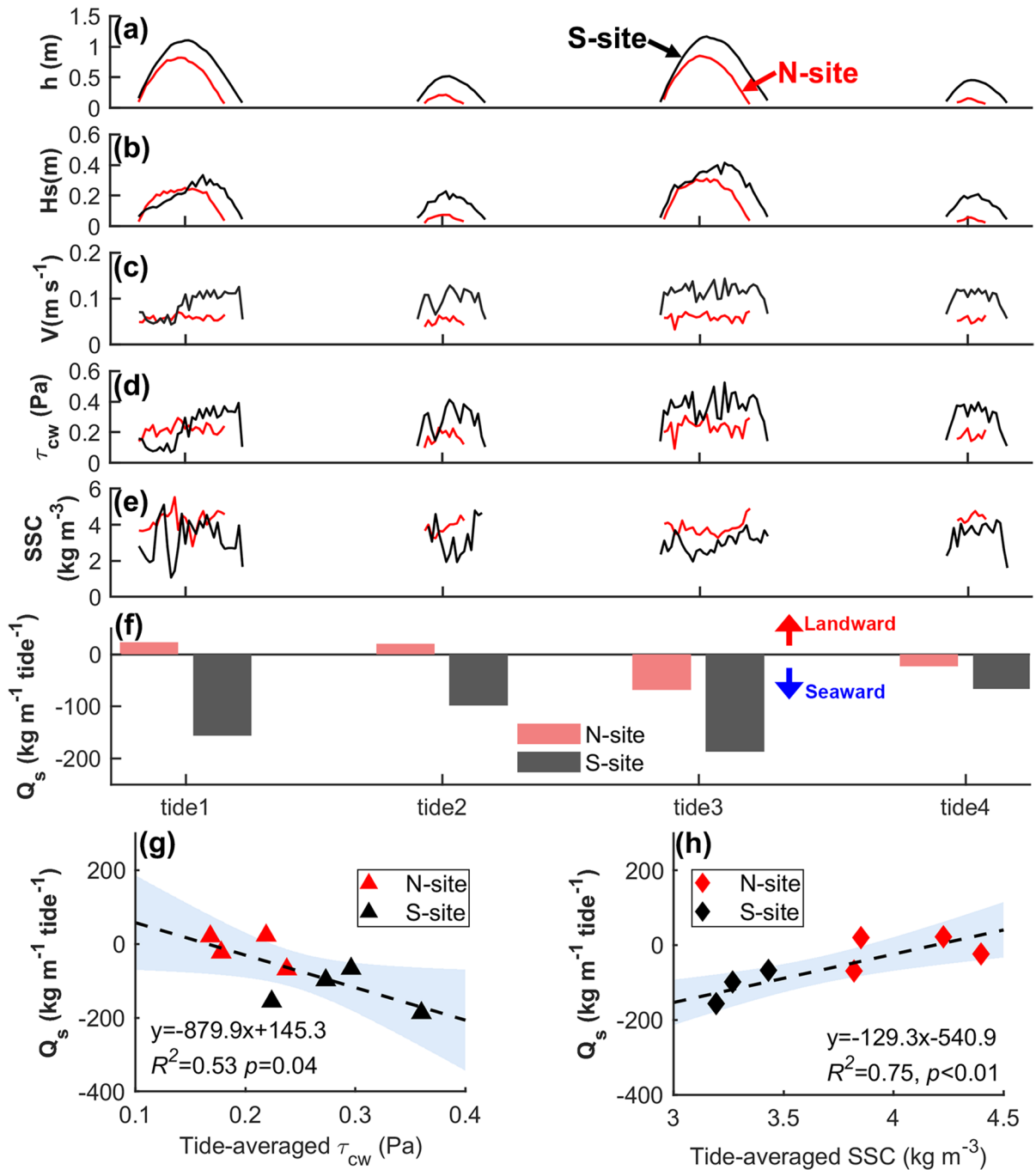
Fig. 5 Comparisons of sediment dynamics between the two marsh edges: **(a)** Water depth (h); **(b)** Significant wave height (H_s); **(c)** Values of flow velocity (V); **(d)** Bed shear stress due to combined wave-current actions (τ_{cw}); **(e)** Suspended sediment concentration (SSC); **(f)** Net sediment flux in four tides (Q_s); **(g)** Relationships between Q_s and tide-averaged τ_{cw}; and **(h)** Relationships between Q_s and tide-averaged SSC. All statistical analysis was finished with the significance level $\alpha = 0.05$

shear stress and consequent bed level changes would act as the force on seedlings at multiple stages, such as seedling settlement (Zhang et al. 2022), seedling anchoring (Zhao et al. 2021c), and seedling growth (Bouma et al. 2009), which facilitated seedling dislodgement and hampered its establishment. It would be challenging for seedling establishment in an environment with low SSC and activated resuspension by high bed shear stress (e.g., S-site in the study).

From the perspectives of landscape changes, we found marsh expansion at the two sites occurred within different spatial extents, as proven by the distance between the initial marsh edge and MNHW (Fig. 4a), also tidal flat area above MNHW (Fig. 4b). Elevations determine the spatial extent of marsh expansion by opening the first "windows of opportunity" (Balke et al. 2014; Hu et al. 2015b; Fivash et al. 2021). Low elevations that result in high inundation frequency lead to seedling death due to physiological stress (Cui et al. 2020; Xue et al. 2020). Sufficient habitats with moderate inundation frequency at N-site helped accommodate new scattered patches, while new marshes at S-site would enlarge in size by merging into the existing ones in the narrow space above MHNW.

Our field-based study gives empirical insights into the shaping role of physical constraints at the site-scale marsh pattern dynamics (Fig. 6a, b). It underlines two key variables: i) disturbance induced by bed shear stress and SSC, and ii) elevation-dependent spatial extent for expansion. Marsh pioneer species tend to select adaptive reproduction strategies to enhance survival in highly disturbed environments (Friess et al. 2012). Unsuitable physical disturbances decrease the possibility of success in sexual reproductions. To increase the population, asexual reproductions with high survival rates (e.g., Minden et al. 2012; Hu et al. 2015a; Silliman et al. 2015) would therefore take over, reducing the effective distance of species spread (Belzile et al. 2010; Liu et al. 2014). This informs that the distance-limited marsh expansion (e.g., infilling and edge expansion) is dominant at the seriously disturbed sites with high bed shear stress, low SSC, sediment resuspension, and bed erosion (Fig. 6b). Moreover, we supported the view that long-distance outlying expansion is more likely to occur at sites with large spatial extent that is sufficiently high in the tidal frame (Fig. 6a). The varying spatial extent often leads to changing biological

responses in landscapes (Holland et al. 2004; Miguet et al. 2016; Martin 2018). At sites with limited spatial extent, such as the S-site in this study, large-scale outlying expansion beyond the initial marsh edges becomes challenging due to the narrow potential habitats available for marsh establishment. In all, the spatially explicit marsh establishment was the consequence of trade-offs among physical disturbance, spatial extent and reproductive traits of marsh pioneer species.

Short-term marsh evolution: a temporal relay racing with opportunities and risks

The distinctly different spatial paradigms of marsh changes between the two sites highlight the significance of outlying expansion, particularly in sustaining salt marshes during storms. Scattered patches at N-site quickly grew through edge expansion (Fig. 3c) and became spatially compact (Fig. 3b), while sparse new patches at S-site were insufficient to support large-scale edge expansion and disappeared during typhoon In-Fa (Fig. 3a). At the patch level, high temperatures in summer steer clonal growth with dense tillers in salt marshes (Nieva et al. 2005). When scaling up to the site level, multiple patches of *Scirpus* tend to coalescence rather than collision (Zhao et al. 2021a). The number of previously established patches contributes to a homogeneous state of marsh cover, enhancing system resilience (Holling 1973) by setting the origin of edge expansion and invoking intraspecific positive feedback (Duggan-Edwards et al. 2020; Huang et al. 2022).

We represented the "relay-racing" spatial processes mentioned above using a conceptual diagram based on our results (Fig. 6c). It simplified marsh growing periods into three stages: establishment (stage I), growth (stage II), and recovery from abrupt events (stage III). Successful establishment at stage I does not immediately promote marsh growth but occupies blank ecological niches through outlying-expansion patches. These dense small patches expand around patch edges at stage II and substantially accelerate marsh growth. If marsh growth at stage II exceeds the threshold during extreme events, the grown marsh patches can persist into stage III (State A in Fig. 6); otherwise, marsh patches may begin to retreat (State B in Fig. 6). As a result, successive effects of landscape configuration settings in marsh establishment and landscape
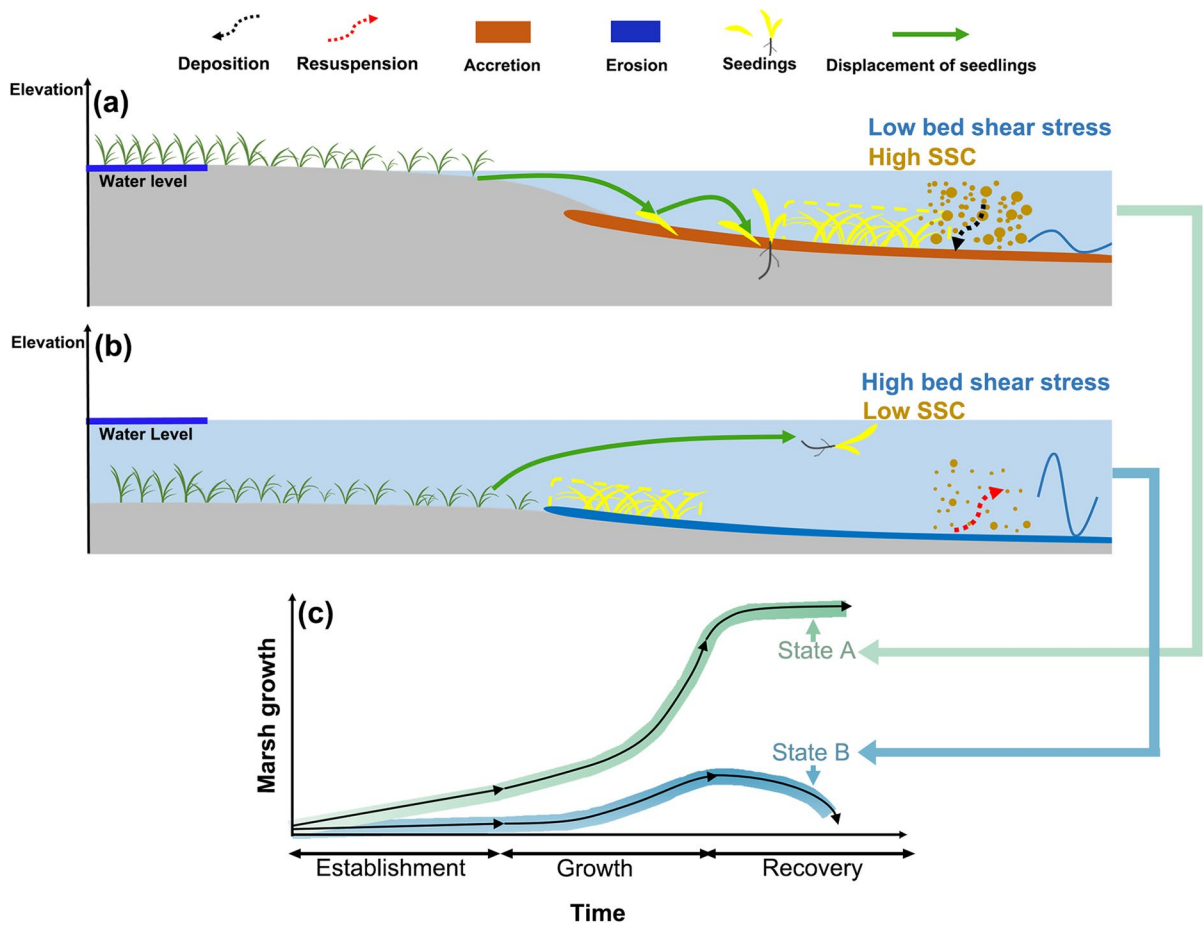
Fig. 6 Conceptual diagrams of different marsh establishment and marsh growth under varying physical conditions: **(a)** Seedling establishment at sites with low bed shear stress, high SSC and large spatial extent; **(b)** Seedling establishment at sites with high bed shear stress, low SSC and narrow spatial extent; **(c)** Different states of short-term marsh evolution, where state A represented net seasonal marsh expansion and state B represented the net seasonal marsh shrink

composition changes in marsh growth finally shape the state of short-term marsh evolution and eventually influence the long-term pattern at inter-annual scale. The former is indispensable and heavily dependent on the magnitude of physical constraints.

It is important to note that opportunities and risks coexist in marsh establishment due to the intrinsic temporal variability of physical forces (Hu et al. 2021; van Belzen et al. 2022). Organism tolerance is enhanced by episodic low disturbances within specific temporally varying cycles. For example, adequate inundation-free periods help stabilize seedlings by forming forked roots (Jiang et al. 2022). Conversely, instantaneous peak hydrodynamics might lift seedlings

off and lead to failures of marsh colonization on mudflats (Poppema et al. 2019). A similar occasion-related mechanism also comes into play when facing typhoon events. The timing, strength and track of typhoons are uncertain (Sobel Adam et al. 2016; Lanzante 2019). Once the population size exceeds the tipping point for maintaining a stable state (Didham et al. 2005; Dakos et al. 2019), the opportunity for marsh survival can be created before typhoons. However, insufficient marsh growth might open "windows of risk" while encountering the "unknown" typhoon (e.g., S-site in the study). Therefore, subtle shifts between opportunities and risks in biophysical processes would facilitate formation of various salt marsh landscapes.

Decreased sediment challenges salt marsh conservation, spanning from monthly or seasonal (Lacy et al. 2020) to annual and decadal (Li et al. 2021) scale. Our results illustrated that low SSC hampers sediment retention near marsh edges (Fig. 5h) and shapes an erosion-prone sedimentary regime (Fig. 4c). Morphological responses to on-shore sediment supply determine the dynamic habitat size for marsh growth by elevating mudflats (Donatelli et al. 2018; Ladd et al. 2019). Sediment starving induces gradual shifts from accretion to erosion and threatens the safety of coastal wetlands by enlarging the drowned areas in mega-delta systems, such as the Yangtze (Yang et al. 2011; van Maren et al. 2013), the Mississippi (Jankowski et al. 2017; Sanks et al. 2020), and the Nile (Alfy Morcos 1995). Global sediment deficits might undermine the positive effect of marsh development and put it at a persistent risk.

Implications for restoration

It is a necessary step to convert risks into opportunities for the success in the practice of salt marsh restoration. We agree with previous studies emphasizing crucial window periods of salt marsh establishment in spring (Hu et al. 2015b; Fivash et al. 2021; Ning et al. 2020). Additionally, we further figured out that marshes should expand as soon as possible in spring to withstand subsequent typhoons in summer. Specific artificial assists can help organisms in coping with physical stress by optimizing their habitats. Auxiliary structures at the patch level, such as mesh bags to reduce loss of sowed seeds (Vanderklift et al. 2020) and mimics to strengthen stems (Temmink et al. 2020) can enhance individual survival. Expanding spatial extent at the site level can be achieved by elevating tidal platforms in front of salt marsh edges with dredged materials (Wiegman et al. 2018; Baptist et al. 2019) in case of insufficient accretions. Bio-based infrastructures on mudflats, such as oyster beds (Chowdhury et al. 2019), can dissipate wave energy, thus accelerating marsh establishment and delivering multiple ecological functions (Dafforn et al. 2015; Gittman et al. 2016).

The findings of this study highlight the significance of site-specific properties in salt marsh evolution. This is highly relevant to design strategies for restoration projects. Choosing the appropriate restoration site can reduce unnecessary costs by harnessing "power from nature" (Cheong et al. 2013; Kumar et al. 2021). Marsh expansion in the accretion-prone site (e.g., N-site in this study) tends to be spatially significant and inherently resilient, primarily due to the robust performance of seedling survival in an accreting environment (Cao et al. 2018). Conversely, the erosion-prone sites (e.g., S-site in this study) are more likely to experience limited seaward marsh expansion and landward marsh migration. Hence, applying uniform measures for marsh restoration at the landscape scale may not be appropriate, even when dealing with the same estuarine system and similar wind exposures. It is advisable to prioritize investments in vulnerable marshes at erosion-prone sites.

Conclusion

The present study has demonstrated that physical constraints drive state differentiations in short-term marsh evolution at the landscape scale. We recognized that the seasonal net marsh expansion started from outlying expansion in spring, followed by edge expansion in summer, and infilling expansion in autumn. In contrast, only distance-limited infilling and edge expansion can be observed when the marsh is in a net seasonal retreat. This finding, combined with comparisons of hydrodynamics, sediment transport, and morphological changes, demonstrates that site-specific physical constraints drive variations in the state of short-term marsh evolution. Marsh development faces significant challenges in seizing fleeting opportunities and mitigating uncertain risks during extreme events and sediment decline. As a result, we propose that prioritizing the restoration of the erosion-prone sites should be the primary focus at the landscape scale. This information would contribute to the increased knowledge of coastal management strategies, especially for other similar mega-delta systems.

Declarations

References

Alfy Morcos F (1995) The Impact of Human Activities on the Erosion and Accretion of the Nile Delta Coast. J Coast Res 11:821–833

Balke T, Herman PMJ, Bouma TJ (2014) Critical transitions in disturbance-driven ecosystems: identifying windows of opportunity for recovery. J Ecology 102:700–708

Baptist MJ, Gerkema T, van Prooijen BC, van Maren DS, van Regteren M, Schulz K, Colosimo I, Vroom J, van Kessel T, Grasmeijer B, Willemsen P, Elschot K, de Groot AV, Cleveringa J, van Eekelen EMM, Schuurman F, de Lange HJ, van Puijenbroek MEB (2019) Beneficial use of dredged sediment to enhance salt marsh development by applying a 'Mud Motor'. Ecol Eng 127:312–323

Bauer JE, Cai WJ, Raymond PA, Bianchi TS, Hopkinson CS, Regnier PAG (2013) The changing carbon cycle of the coastal ocean. Nature 504:61–70

Belzile F, Labbé J, LeBlanc MC, Lavoie C (2010) Seeds contribute strongly to the spread of the invasive genotype of the common reed (*Phragmites australis*). Biol Invasions 12:2243–2250

Berling-Wolff S, Wu J (2004) Modeling urban landscape dynamics: A case study in Phoenix, USA. Urban Ecosyst 7:215–240

Bouma TJ, Friedrichs M, Klaassen P, van Wesenbeeck BK, Brun FG, Temmerman S, van Katwijk MM, Graf G, Herman PMJ (2009) Effects of shoot stiffness, shoot size and current velocity on scouring sediment from around seedlings and propagules. Mar Ecol Prog Ser 388:293–297

Bouma TJ, van Belzen J, Balke T, van Dalen J, Klaassen P, Hartog AM, Callaghan DP, Hu Z, Stive MJF, Temmerman S, Herman PMJ (2016) Short-term mudflat dynamics drive long-term cyclic salt marsh dynamics. Limnol Oceanogr 61:2261–2275

Cao H, Zhu Z, Balke T, Zhang L, Bouma TJ (2018) Effects of sediment disturbance regimes on *Spartina* seedling establishment: Implications for salt marsh creation and restoration. Limnol Oceanogr 63:647–659

Cheong SM, Silliman B, Wong PP, van Wesenbeeck B, Kim CK, Guannel G (2013) Coastal adaptation with ecological engineering. Nat Clim Change 3:787–791

Chowdhury MSN, Walles B, Sharifuzzaman SM, Shahadat Hossain M, Ysebaert T, Smaal AC (2019) Oyster breakwater reefs promote adjacent mudflat stability and salt marsh growth in a monsoon dominated subtropical coast. Sci Rep 9:8549

Church JA, White NJ (2011) Sea-Level Rise from the Late 19th to the Early 21st Century. Surv Geophys 32:585–602

Costanza R, d'Arge R, de Groot R, Farber S, Grasso M, Hannon B, Limburg K, Naeem S, O'Neill RV, Paruelo J, Raskin RG, Sutton P, van den Belt M (1997) The value of the world's ecosystem services and natural capital. Nature 387:253–260

Cui L, Yuan L, Ge Z, Cao H, Zhang L (2020) The impacts of biotic and abiotic interaction on the spatial pattern of salt marshes in the Yangtze Estuary. China Estuar Coast Shelf Sci 238:106717

Dafforn KA, Glasby TM, Airoldi L, Rivero NK, Mayer-Pinto M, Johnston EL (2015) Marine urbanization: an ecological framework for designing multifunctional artificial structures. Front Ecol Environ 13:82–90

Dai Z (2021) Changjiang Riverine and Estuarine Hyrdo-morphodynamic processes: in the Context of Anthropocene Era. Springe Singapore, Singapore

Dakos V, Matthews B, Hendry AP, Levine J, Loeuille N, Norberg J, Nosil P, Scheffer M, De Meester L (2019) Ecosystem tipping points in an evolving world. Nat Ecol Evol 3:355–362

de Groot R, Brander L, van der Ploeg S, Costanza R, Bernard F, Braat L, Christie M, Crossman N, Ghermandi A, Hein L, Hussain S, Kumar P, McVittie A, Portela R, Rodriguez LC, ten Brink P, van Beukering P (2012) Global

estimates of the value of ecosystems and their services in monetary units. Ecosyst Serv 1:50–61

Debnath K, Chaudhuri S (2011) Effect of suspended sediment concentration on local scour around cylinder for clay-sand mixed sediment beds. Eng Geol 117:236–245

Didham RK, Watts CH, Norton DA (2005) Are systems with strong underlying abiotic regimes more likely to exhibit alternative stable states? Oikos 110:409–416

Donatelli C, Ganju NK, Zhang X, Fagherazzi S, Leonardi N (2018) Salt Marsh Loss Affects Tides and the Sediment Budget in Shallow Bays. J Geophys Res Earth Surf 123:2647–2662

Duggan-Edwards MF, Pagès JF, Jenkins SR, Bouma TJ, Skov MW (2020) External conditions drive optimal planting configurations for salt marsh restoration. J Appl Ecol 57:619–629

Fivash GS, Temmink RJM, D'Angelo M, van Dalen J, Lengkeek W, Didderen K, Ballio F, van der Heide T, Bouma TJ (2021) Restoration of biogeomorphic systems by creating windows of opportunity to support natural establishment processes. Ecol Appl 31:e02333

Folkard AM (2019) Biophysical Interactions in Fragmented Marine Canopies: Fundamental Processes, Consequences, and Upscaling. Front Mar Sci 6:279

Forman RTT (1995) Land mosaics: the ecology of landscapes and regions. Cambridge Univ Press, Cambridge

Friess DA, Krauss KW, Horstman EM, Balke T, Bouma TJ, Galli D, Webb EL (2012) Are all intertidal wetlands naturally created equal? Bottlenecks, thresholds and knowledge gaps to mangrove and saltmarsh ecosystems. Biol Rev 87:346–366

Ge Z-M, Li S-H, Tan L-S, Li Y-L, Hu Z-J (2019) The importance of the propagule-sediment-tide "power balance" for revegetation at the coastal frontier. Ecol Appl 29(7):e01967

Gittman RK, Peterson CH, Currin CA, Joel Fodrie F, Piehler MF, Bruno John F (2016) Living shorelines can enhance the nursery role of threatened estuarine habitats. Ecol Appl 26:249–263

Group of Shanghai Island Investigation (GSII) (1996) Report of Shanghai Island Comprehensive Investigation. Shanghai Scientific and Technological Press, Shanghai (in Chinese)

Guo L, Su N, Townend I, Wang ZB, Zhu C, Wang X, Zhang Y, He Q (2019) From the headwater to the delta: A synthesis of the basin-scale sediment load regime in the Changjiang River. Earth-Sci Rev 197:102900

Hanley ME, Bouma TJ, Mossman HL (2020) The gathering storm: optimizing management of coastal ecosystems in the face of a climate-driven threat. Ann Bot 125:197–212

Hoffhine Wilson E, Hurd JD, Civco DL, Prisloe MP, Arnold C (2003) Development of a geospatial model to quantify, describe and map urban growth. Remote Sens Environ 86:275–285

Holland JD, Bert DG, Fahrig L (2004) Determining the Spatial Scale of Species' Response to Habitat. Bioscience 54:227–233

Holling CS (1973) Resilience and Stability of Ecological Systems. Annu Rev Ecol Evol S 4:1–23

Hu Z-J, Ge Z-M, Ma Q, Zhang Z-T, Tang C-D, Cao H-B, Zhang T-Y, Li B, Zhang L-Q (2015a) Revegetation of a native species in a newly formed tidal marsh under varying hydrological conditions and planting densities in the Yangtze Estuary. Ecol Eng 83:354–363

Hu Z, Borsje BW, van Belzen J, Willemsen PWJM, Wang H, Peng Y, Yuan L, De Dominicis M, Wolf J, Temmerman S, Bouma TJ (2021) Mechanistic modeling of marsh seedling establishment provides a positive outlook for coastal wetland restoration under global climate change. Geophys Res Lett 48:e2021GL095596

Hu Z, van Belzen J, van der Wal D, Balke T, Wang ZB, Stive M, Bouma TJ (2015b) Windows of opportunity for salt marsh vegetation establishment on bare tidal flats: The importance of temporal and spatial variability in hydro-dynamic forcing. J Geophys Res Biogeo 120:1450–1469

Huang H, Xu C, Liu Q-X (2022) 'Social distancing' between plants may amplify coastal restoration at early stage. J Appl Ecol 59:188–198

Jankowski KL, Törnqvist TE, Fernandes AM (2017) Vulnerability of Louisiana's coastal wetlands to present-day rates of relative sea-level rise. Nat Commun 8:14792

Jiang C, Li X-Z, Xue L-M, Yan Z-Z, Liang X, Chen X-C (2022) Pioneer salt marsh species *Scirpus mariqueter* disperses quicker in summer with seed contribution from current and last year. Estuar Coast Shelf Sci 264:107682

Kirwan ML, Megonigal JP (2013) Tidal wetland stability in the face of human impacts and sea-level rise. Nature 504:53–60

Kirwan ML, Mudd SM (2012) Response of salt-marsh carbon accumulation to climate change. Nature 489:550–553

Kondolf GM, Gao Y, Annandale GW, Morris GL, Jiang E, Zhang J, Cao Y, Carling P, Fu K, Guo Q, Hotchkiss R, Peteuil C, Sumi T, Wang H-W, Wang Z, Wei Z, Wu B, Wu C, Yang CT (2014) Sustainable sediment management in reservoirs and regulated rivers: Experiences from five continents. Earth's Future 2:256–280

Kumar P, Debele SE, Sahani J, Rawat N, Marti-Cardona B, Alfieri SM, Basu B, Basu AS, Bowyer P, Charizopoulos N, Gallotti G, Jaakko J, Leo LS, Loupis M, Menenti M, Mickovski SB, Mun S-J, Gonzalez-Ollauri A, Pfeiffer J, Pilla F, Pröll J, Rutzinger M, Santo MA, Sannigrahi S, Spyrou C, Tuomenvirta H, Zieher T (2021) Nature-based solutions efficiency evaluation against natural hazards: Modelling methods, advantages and limitations. Sci Total Environ 784:147058

Lacy JR, Foster-Martinez MR, Allen RM, Ferner MC, Callaway JC (2020) Seasonal variation in sediment delivery across the bay-marsh interface of an estuarine salt marsh. J Geophys Res Oceans 125:e2019JC015268

Ladd CJT, Duggan-Edwards MF, Bouma TJ, Pagès JF, Skov MW (2019) Sediment Supply Explains Long-Term and Large-Scale Patterns in Salt Marsh Lateral Expansion and Erosion. Geophys Res Lett 46:11178–11187

Lanzante JR (2019) Uncertainties in tropical-cyclone translation speed. Nature 570:E6–E15

Leonardi N, Carnacina I, Donatelli C, Ganju NK, Plater AJ, Schuerch M, Temmerman S (2018) Dynamic interactions between coastal storms and salt marshes: A review. Geomorphology 301:92–107

Leonardi N, Mei X, Carnacina I, Dai Z (2021) Marine sediment sustains the accretion of a mixed fluvial-tidal delta. Mar Geol 438:106520

Li S-H, Ge Z-M, Xin P, Tan L-S, Li Y-L, Xie L-N (2021) Interactions between biotic and abiotic processes determine biogeomorphology in Yangtze Estuary coastal marshes: Observation with a modeling approach. Geomorphology 395:107970

Li X, Bellerby R, Craft C, Widney SE (2018) Coastal wetland loss, consequences, and challenges for restoration. Anthropocene Coasts 1:1–15

Liu H, Lin Z, Qi X, Zhang M, Yang H (2014) The relative importance of sexual and asexual reproduction in the spread of *Spartina alterniflora* using a spatially explicit individual-based model. Ecol Res 29:905–915

Liu X, Li X, Chen Y, Tan Z, Li S, Ai B (2010) A new landscape index for quantifying urban expansion using multi-temporal remotely sensed data. Landscape Ecol 25:671–682

Luan HL, Ding PX, Wang ZB, Yang SL, Lu JY (2018) Morphodynamic impacts of large-scale engineering projects in the Yangtze River delta. Coast Eng 141:1–11

Mariotti G, Carr J (2014) Dual role of salt marsh retreat: Long-term loss and short-term resilience. Water Resour Res 50(4):2963–2974

Martin AE (2018) The Spatial Scale of a Species' Response to the Landscape Context Depends on which Biological Response You Measure. Curr Landscape Ecol Rep 3:23–33

Miguet P, Jackson HB, Jackson ND, Martin AE, Fahrig L (2016) What determines the spatial extent of landscape effects on species? Landscape Ecol 31:1177–1194

Minden V, Andratschke S, Spalke J, Timmermann H, Kleyer M (2012) Plant trait-environment relationships in salt marshes: Deviations from predictions by ecological concepts. Perspect Plant Ecol 14:183–192

Moffett KB, Gorelick SM, McLaren RG, Sudicky EA (2012) Salt marsh ecohydrological zonation due to heterogeneous vegetation-groundwater-surface water interactions. Water Resour Res 48:W02516

Nieva FJJ, Castellanos EM, Castillo JM, Enrique Figueroa M (2005) Clonal growth and tiller demography of the invader cordgrass *Spartina densiflora* brongn At two contrasting habitats in SW European salt marshes. Wetlands 25:122–129

Ning Z, Chen C, Xie T, Wang Q, Bai J, Shao D, Man Y, Cui B (2020) Windows of opportunity for smooth cordgrass landward invasion to tidal channel margins: The importance of hydrodynamic disturbance to seedling establishment. J Environ Manage 266:110559

Panagiotopoulos I, Voulgaris G, Collins MB (1997) The influence of clay on the threshold of movement of fine sandy beds. Coast Eng 32:19–43

Perry GLW (2002) Landscapes, space and equilibrium: shifting viewpoints. Prog Phys Geog 26:339–359

Poirier E, van Proosdij D, Milligan TG (2017) The effect of source suspended sediment concentration on the sediment dynamics of a macrotidal creek and salt marsh. Cont Shelf Res 148:130–138

Poppema DW, Willemsen PWJM, de Vries MB, Zhu Z, Borsje BW, Hulscher SJMH (2019) Experiment-supported modelling of salt marsh establishment. Ocean Coast Manage 168:238–250

Sanks KM, Shaw JB, Naithani K (2020) Field-based estimate of the sediment deficit in coastal Louisiana. J Geophs Res Earth Surf 125:e2019JF005389

Schuerch M, Dolch T, Reise K, Vafeidis AT (2014) Unravelling interactions between salt marsh evolution and sedimentary processes in the Wadden Sea (southeastern North Sea). Prog Phys Geog 38:691–715

Schuerch M, Spencer T, Temmerman S, Kirwan ML, Wolff C, Lincke D, McOwen CJ, Pickering MD, Reef R, Vafeidis AT, Hinkel J, Nicholls RJ, Brown S (2018) Future response of global coastal wetlands to sea-level rise. Nature 561:231–234

Silliman BR, Schrack E, He Q, Cope R, Santoni A, van der Heide T, Jacobi R, Jacobi M, van de Koppel J (2015) Facilitation shifts paradigms and can amplify coastal restoration efforts. P Natl Acad Sci Usa 112:14295

Sobel Adam H, Camargo Suzana J, Hall Timothy M, Lee C-Y, Tippett Michael K, Wing Allison A (2016) Human influence on tropical cyclone intensity. Science 353:242–246

Stein A, Gerstner K, Kreft H (2014) Environmental heterogeneity as a universal driver of species richness across taxa biomes and spatial scales. Ecol Lett 17:866–880

Syvitski JPM, Vörösmarty CJ, Kettner AJ, Green P (2005) Impact of Humans on the Flux of Terrestrial Sediment to the Global Coastal Ocean. Science 308:376–380

Temmerman S, Meire P, Bouma TJ, Herman PMJ, Ysebaert T, De Vriend HJ (2013) Ecosystem-based coastal defence in the face of global change. Nature 504:79–83

Temmink RJM, Christianen MJA, Fivash GS, Angelini C, Boström C, Didderen K, Engel SM, Esteban N, Gaeckle JL, Gagnon K, Govers LL, Infantes E, van Katwijk MM, Kipson S, Lamers LPM, Lengkeek W, Silliman BR, van Tussenbroek BI, Unsworth RKF, Yaakub SM, Bouma TJ, van der Heide T (2020) Mimicry of emergent traits amplifies coastal restoration success. Nat Commun 11:3668

van Belzen J, Fivash GS, Hu Z, Bouma TJ, Herman PMJ (2022) A probabilistic framework for windows of opportunity: the role of temporal variability in critical transitions. J R Soc Interface 19:20220041

van Belzen J, van de Koppel J, Kirwan ML, van der Wal D, Herman PMJ, Dakos V, Kéfi S, Scheffer M, Guntenspergen GR, Bouma TJ (2017) Vegetation recovery in tidal marshes reveals critical slowing down under increased inundation. Nat Commun 8:15811

van de Koppel J, Bouma TJ, Herman PMJ (2012) The influence of local- and landscape-scale processes on spatial self-organization in estuarine ecosystems. J Exp Biol 215:962–967

van Maren DS, Yang S-L, He Q (2013) The impact of silt trapping in large reservoirs on downstream morphology: the Yangtze River. Ocean Dynam 63:691–707

van Wesenbeeck BK, van de Koppel J, Herman PMJ, Bertness MD, van der Wal D, Bakker JP, Bouma TJ (2008) Potential for Sudden Shifts in Transient Systems: Distinguishing Between Local and Landscape-Scale Processes. Ecosystems 11:1133–1141

Vanderklift MA, Doropoulos C, Gorman D, Leal l, Minne AJP, Statton J, Steven ADL, Wernberg T, (2020) Using propagules to restore coastal marine ecosystems. Front Mar Sci 7:724

Vasseur DA, DeLong JP, Gilbert B, Greig HS, Harley CDG, McCann KS, Savage V, Tunney TD, O'Connor MI (2014) Increased temperature variation poses a greater risk to species than climate warming. P Roy Soc B-Biol Sci 281:20132612

Wang C, Temmerman S (2013) Does biogeomorphic feedback lead to abrupt shifts between alternative landscape states?: An empirical study on intertidal flats and marshes. J Geophys Res Earth Surf 118:229–240

Wang H, Ge Z, Yuan L, Zhang L (2014) Evaluation of the combined threat from sea-level rise and sedimentation reduction to the coastal wetlands in the Yangtze Estuary, China. Ecol Eng 71:346–354

Wang X, Wang W, Tong C (2016) A review on impact of typhoons and hurricanes on coastal wetland ecosystems. Acta Ecol Sin 36:23–29

Wei W, Zhou Y, Tian B, Qian W, Zhan Y, Huang G (2018) Topography Retrieval on Typical Salt Marsh of Coastal Zone Based on Terrestrial Laser Scanning. J Jilin Univ Earth Sci Ed 48:1889–1897 (in Chinese with English abstract)

Wiegman ARH, Day JW, D'Elia CF, Rutherford JS, Morris JT, Roy ED, Lane RR, Dismukes DE, Snyder BF (2018) Modeling impacts of sea-level rise, oil price, and management strategy on the costs of sustaining Mississippi delta marshes with hydraulic dredging. Sci Total Environ 618:1547–1559

Willemsen PWJM, Smits BP, Borsje BW, Herman PMJ, Dijkstra JT, Bouma TJ, Hulscher SJMN (2022) Modelling decadal salt marsh development: variability of the salt marsh edge under influence of waves and sediment availability. Water Resour Res 58:e2020WR028962

Winterwerp JC (2001) Stratification effects by cohesive and noncohesive sediment. J Geophys Res Oceans 106:22559–22574

Woodruff JD, Irish JL, Camargo SJ (2013) Coastal flooding by tropical cyclones and sea-level rise. Nature 504:44–52

Xie W, He Q, Zhang K, Guo L, Wang X, Shen J, Cui Z (2017) Application of terrestrial laser scanner on tidal flat morphology at a typhoon event timescale. Geomorphology 292:47–58

Xu C, Liu M, Zhang C, An S, Yu W, Chen JM (2007) The spatiotemporal dynamics of rapid urban growth in the Nanjing metropolitan region of China. Landscape Ecol 22:925–937

Xue L, Jiang J, Li X, Yan Z, Zhang Q, Ge Z, Tina B, Craft C (2020) Salinity affects topsoil organic carbon concentrations through regulating vegetation structure and productivity. J Geophys Res Biogeo 125:e2019JG005217

Yang S, Li M, Dai S, Liu Z, Zhang J, Ding P (2006) Drastic decrease in sediment supply from the Yangtze River and its challenge to coastal wetland management. Geophys Res Lett 33:L06408

Yang SL, Luo X, Temmerman S, Kirwan M, Bouma T, Xu K, Zhang S, Fan J, Shi B, Yang H, Wang YP, Shi X, Gao S (2020) Role of delta-front erosion in sustaining salt marshes under sea-level rise and fluvial sediment decline. Limnol Oceanogr 65:1990–2009

Yang SL, Milliman JD, Li P, Xu K (2011) 50,000 dams later: Erosion of the Yangtze River and its delta. Global Planet Change 75:14–20

Yuan L, Chen Y-H, Wang H, Cao H-B, Zhao Z-Y, Tang C-D, Zhang L-Q (2020) Windows of opportunity for salt marsh establishment: the importance for salt marsh restoration in the Yangtze Estuary. Ecosphere 11:e03180

Yuan Y, Li X, Xie Z, Xue L, Yang B, Zhao W, Craft CB (2022) Annual Lateral Organic Carbon Exchange Between Salt Marsh and Adjacent Water: A Case Study of East Headland Marshes at the Yangtze Estuary. Front Mar Sci 8:2090

Zhang J, Yuan L, Cao H, Yang L, Zhao Z, Wang X, Zhang L (2022) Study on the critical shear stress of floating initiation for the seeds and seedlings of intertidal salt marsh plants. Acta Ecol Sin 42:1821–1829 (in Chinese with English abstract)

Zhang Q-H, Yan B, Wai OWH (2009) Fine sediment carrying capacity of combined wave and current flows. Int J Sediment Res 24:425–438

Zhao C, Mao Z, Yu Z, Xu H, Li J (2008) The Analysis of the Eastern Chongming Tidal Flats Evolution in the Yangtze River Estuary. Trans Oceanol Limnol 3:27–34 (in Chinese with English abstract)

Zhao L-X, Zhang K, Siteur K, Li X-Z, Liu Q-X, van de Koppel J (2021a) Fairy circles reveal the resilience of self-organized salt marshes. Sci Adv 7:eabe1100

Zhao Z, Zhang L, Li X, Yuan L, Bouma TJ (2021b) The onset of secondary seed dispersal is controlled by germination-features: A neglected process in sudden saltmarsh establishment. Limnol Oceanogr 66:3070–3084

Zhao Z, Zhang L, Yuan L, Bouma TJ (2021c) Saltmarsh seeds in motion: the relative importance of dispersal units and abiotic conditions. Mar Ecol Prog Ser 678:63–79

Zhu Q (2017) Sediment dynamics on intertidal mudflats: A study based on in situ measurements and numerical modelling. PhD Thesis, Delft University of Technology

Zhu Z, van Belzen J, Zhu Q, van de Koppel J, Bouma TJ (2020) Vegetation recovery on neighboring tidal flats forms an Achilles' heel of saltmarsh resilience to sea level rise. Limnol Oceanogr 65:51–62